MJFAS
Malaysian Journal of Fundamental and Applied Sciences

Hao *et al.* | Malaysian Journal of Fundamental and Applied Sciences, Vol. 22 (2026) 61–72

RESEARCH ARTICLE

Fractional Analysis of Magnetic non-Newtonian Casson Fluid with Copper Nanoparticles Through Inclined Stenosed Artery

Chan Wai Hao[a,*], Dzuliana Fatin Jamil[a], Salah Uddin[b], Norhaliza Abu Bakar[c], Rozaini Roslan[d]

[a]Department of Mathematical Sciences, Faculty of Science, Universiti Teknologi Malaysia, 81310 UTM Johor Bahru, Johor, Malaysia; [b]Department of Humanities & Science, College of Aeronautical Engineering, National University of Sciences & Technology, Risalpur, 23200, Pakistan; [c]Centre for Diploma Studies, Universiti Tun Hussein Onn Malaysia, Pagoh Campus, 84600 Muar, Johor, Malaysia; [d]Faculty of Applied Sciences and Technology, Universiti Tun Hussein Onn Malaysia, Pagoh Campus, 84600 Muar, Johor, Malaysia

Abstract Cardiovascular diseases include various heart and blood vessel disorders. Arterial stenosis, caused by the buildup of fatty deposits and other materials, narrows arteries and disrupts normal blood flow, leading to increased wall shear stress and flow disturbances. In this study, the Caputo-Fabrizio fractional derivative is applied to analyze blood flow with copper nanoparticles in an inclined stenosed artery. Blood is modeled as a non-Newtonian Casson fluid under a uniform magnetic field and pressure gradient. Using the Laplace and Hankel transform techniques, analytical solutions for blood and magnetic particle velocities are obtained, and the effects of flow parameters, Hartmann number, time, Casson fluid parameter, and fractional order are presented graphically. Validation against limiting cases shows good agreement with previous studies. The results demonstrate that blood and particle velocities increase with fractional order, time, and Casson fluid parameter, but decrease with higher Hartmann number, with blood velocity generally exceeding particle velocity. These findings are useful for designing targeted drug delivery systems by understanding the behavior of non-Newtonian nanofluids in stenosed arteries under magnetic fields.

Keywords: Caputo-Fabrizio, Casson fluid, Magnetic field, Copper Nanoparticles, Inclined stenosed artery.

***For correspondence:**
chanwaihao1030@gmail.com

Received: 5 August 2025
Accepted: 22 Dec. 2025

Introduction

Understanding the mechanics of physiological fluid, especially blood play an important role for identifying and treatment of various disease states. From past to the present, researchers committed to investigate the areas related to blood flow in blood vessels especially stenosed artery [1] . The term atherosclerosis is closely related to stenosed artery and major factor of cardiovascular diseases such as coronary artery disease (CAD), peripheral artery disease (PAD) and carotid artery disease [2, 3]. Therefore, understanding the mechanical effects that arteries on the blood flow is particularly challenging as the diverse and anisotropic behaviour of arterial wall that composed by varying biomechanical properties. While numerous mathematical models have been developed, they often simplify the complex geometry of the human vasculature by assuming arteries are perfectly horizontal or vertical. However, in reality, blood vessels are frequently oriented at various angles within the body. [4] provide an overview of how the degree of stenosis influence blood flow behaviour in an overlapping stenosis. [5] numerically analyses flow variations in inclined stenosed arteries under condition of resting and exercise with existence of external body acceleration. Therefore, investigating blood flow in inclined stenosed arteries

is a crucial step toward developing more accurate and clinically relevant biomechanical models that can better predict hemodynamic stresses and disease progression [6-7].

The interaction between blood flow and magnetic fields represents an intriguing area linking biology, medicine, and physics. Blood flow can be affected by magnetic fields because red blood cells contain iron rich haemoglobin, which gives blood weak magnetic properties. When a magnetic field is applied, it creates a resistive Lorentz force that slows down the movement of blood. This idea makes it possible to treat stenotic arteries using targeted therapies and non-invasive treatments [8-11]. The use of magnetic field to regulate blood flow is being actively investigated by the developing field of bio-magnetic fluid dynamics. This might be done to modulate circulation during surgical procedures or to direct magnetic drug carriers to particular locations [12, 13], [14] studied the effect of magnetic field on blood flow through an inclined cylindrical tube and conclude that the blood velocities are reduced by the magnetic field while the blood flow was improved by the gradually inclination angle.

Understanding the mechanics of blood flow is crucial for diagnosing and treating diseases, as different types of fluid models require distinct mathematical and biomechanical approaches. Since the viscosity of non-Newtonian fluids depends on shear rate or stress, blood flow in a narrow artery is treated as non-Newtonian due to large variations in shear rate caused by the stenosis. [15] conducted a study of non-Newtonian models for more than a single layer blood flow in stenosis arteries. In this study, Casson fluid model will be the targeted model to demonstrate the blood flow in confined artery. Casson fluid model is a non-Newtonian fluid model with yield stress has been widely used for modelling certain physiological fluids in order to investigate the effect external force on them. [16] investigated the effect of non-Newtonian Casson blood flow for through a symmetric stenosed artery. In the stenosis section, the Casson fluid model could adequately exhibit the characteristics of blood flow through a constricted artery, such as low shear rates. Blood exhibits non-Newtonian characteristics during the low shear rate environment of a stenosed artery [17]. The Casson fluid model effectively shows how blood behaves in a narrowed artery because it includes the idea of yield stress which is the least amount of shear stress needed for the fluid to start flowing [18-20].

Nanomedicine applies nanoscale technologies to improve healthcare by enhancing disease detection, treatment, and monitoring. Applications of nanoparticles are transforming modern medicine and offering innovative solutions to complex heath challenges. With growing maturity, nanomedicine and nanotechnology are increasingly being developed for blood vessel therapies. This rapidly advancing field has the potential to transform healthcare by offering more accurate and less invasive methods. [21] studied the effect of magnetic nanoparticles between gold and copper on drug delivery in a tapered stenosed artery using non-Newtonian fluid. [22] investigated the copper nanoparticles suspended in blood transported thermally through a non-uniform wavy channel and found that nanoparticles contribute to slow down fluid flow and increase temperature. The suspension of nanoparticles in a base fluid or called nanofluid can significantly enhance thermal conductivity [23]. To examine treatment potential, copper nanoparticles are implemented into the model. Copper nanoparticles are selected due to their established use in vascular disorders and power to alter the thermophysical properties of blood [24, 25]. The integration of magnetic nanoparticles into blood flow models is a key area of contemporary research and focus on applications like magnetically targeted drug delivery [26].

To capture the complex and time-dependent behaviour of blood flow, advanced mathematical tools are required. The unique features of the Caputo-Fabrizio fractional derivative include a non-singular kernel, memory effect, and simplicity in the initial condition of a problem, making it simple and more flexible than other fractional derivatives. [27] reported the fractional differential equations like Caputo-Fabrizio fractional derivative could be effectively utilized for drug concentration modelling. In this context, the study is very beneficial to understand the concentration of drug particles for drug delivery application in biomedicine. [28] studied the effect of Caputo-Fabrizio toward the Casson fluid in a microchannel and conclude that when compared to regular fluid behaviour, the Caputo- Fabrizio fractional derivative obviously the better option for enhancing fluid motion. Caputo-Fabrizio fractional derivative is the modification of the Caputo derivative to describe memory effects without a singular kernel and offer a distinct advantage over classical fractional derivatives that have singularities [29]. This non-singular method offers a more reliable and biologically accurate framework for explaining the memory-dependent and viscosity characteristics of blood flow, particularly when examining the short-term impacts of magnetic fields and interactions between nanoparticles in a stenosed artery [30-32].

Many studies have explored the use of various nanoparticles such as gold or silver, yet limited attention has been given to copper nanoparticles in blood flow analysis particularly within inclined stenosed arteries. This gap is important because incorporating copper nanoparticles into blood flow models can provide a more realistic representation of nanoparticle-based biomedical applications. To address this,

the present study develops a fractional mathematical model for unsteady Casson blood flow containing copper nanoparticles in an inclined stenosed artery, employing the Caputo–Fabrizio fractional derivative. The study aims to analyse copper nanoparticle blood flow under a uniformly distributed magnetic field and provides a detailed graphical analysis of various parameters to capture the precise mathematical behavior of the flow.

Formulation of the Problem

The Casson copper nanofluid flow is axially symmetric, and both location along the axial distance (z) and height of the stenosis rise with the blood vessel's radius.

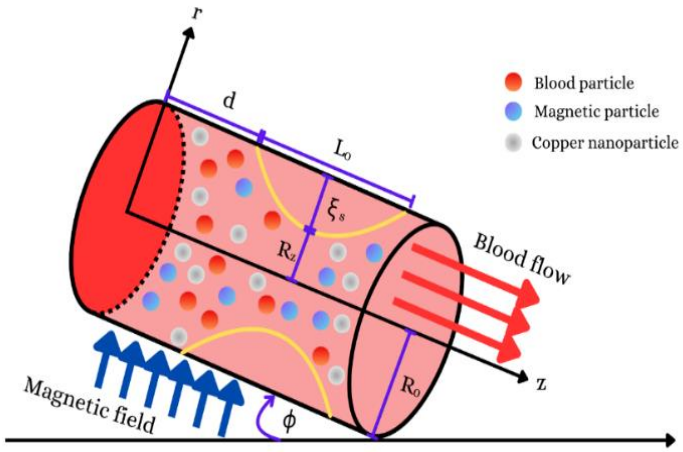

Figure 1: Geometry of magnetic blood flow with copper nanoparticles in an inclined artery.

The linearized magnetohydrodynamics force is expressed as:

$$\vec{J} \times \vec{B} = \sigma\left(\vec{E} + \vec{V} \times \vec{B}\right) \times \vec{B} = -\sigma B^2 u(r,t)\vec{j}, \tag{1}$$

where $\vec{j}$, is the unit vector in z- direction. According to Newton's second law of motion, the force due to the motion between blood and magnetic particle is defined as:

$$m\frac{\partial v(r,t)}{\partial t} = K_m[u(r,t) - v(r,t)], \tag{2}$$

The pressure gradient of the blood flow is represented as: The governing equation of blood flow in the inclined cylinder polar coordinates with presence of pressure gradient and magnetic field is provided as:

$$-\frac{\partial p}{\partial z} = A_0 + A_1 \cos\left(\omega_\rho t\right). \tag{3}$$

The governing equation of blood flow in the inclined cylinder polar coordinates with presence of pressure gradient and magnetic field is provided as:

$$\rho_{nf}\frac{\partial u(r,t)}{\partial t} = (A_0 + A_1\cos(\omega_p t) + \mu_{nf}\left[1 + \frac{1}{\beta}\right]\left[\frac{\partial^2 \mathrm{u(r,t)}}{\partial r^2} + \frac{1}{\mathrm{r}}\frac{\partial \mathrm{u(r,t)}}{\partial r}\right]$$
$$+KN[v(r,t) - u(r,t)] - \sigma_{nf}B^2 u(r,t)sin\theta + gsin\phi, \tag{4}$$

where A_0 is the constant of the pressure gradient and $A_1$is the amplitude of the fluctuating component of pressure gradient which is considered for systolic and diastolic pressures. Whereas the motion of magnetic particles of the blood flow is as follow:

$$m\frac{\partial v(r,t)}{\partial t} = K[u(r,t) - v(r,t)], \tag{5}$$

where $u(r,t)\ and\ v(r,t)$ represented the blood flow and magnetic particles velocity along the axis direction respectively and m is the magnetic particles average mass, ρ_{nf} is the density of the nanofluid. The blood flow inside a circular cylinder with radius R_0 has the following initial and boundary conditions:

$$u(r,0) = 0, v(r,0) = 0, r \in [0, R_0]\ ,$$
$$u(R_0,t) = 0, v(R_0,0) = 0, t > 0\ . \tag{6}$$

Table 1 indicates the thermophysical properties associated with Casson nanofluids [33]. The following dimensionless terms are introduced for parameter rescaling shown as:

$$r^* = \frac{r}{R_0}\ ,\ t^* = \frac{tv}{{R_0}^2}\ ,u^* = \frac{u}{u_0}\ ,v^* = \frac{v}{u_0}\ ,g^* = \frac{g}{{u_0}^2/R_0},$$
$$z^* = \frac{z_0}{R_0}, p^* = \frac{pR_0}{\mu u_0}. \tag{7}$$

The summation of the non-dimensional governing equation (after dropping dashes) can be obtained by inserting the non-dimensional parameter in (7) into each term of equation (4) to (5). The Caputo-Fabrizio order model is expressed as:

$$D_t^{\alpha}u(r,t) = A_2 + A_3\cos(\omega_p t) + \beta_1\left[\frac{\partial^2 \mathrm{u}(\mathrm{r},\mathrm{t})}{\partial r^2} + \frac{1}{\mathrm{r}}\frac{\partial \mathrm{u}(\mathrm{r},\mathrm{t})}{\partial r}\right]$$
$$+R[v(r,t) - u(r,t)] - Ha^2u(r,t) + \frac{sin\phi}{F}, A_0 > 0, \tag{8}$$

$$GD_t^{\alpha}v(r,t) = \mathrm{u}(r,t) - v(r,t), \tag{9}$$

with the related dimensionless initial and boundary conditions:

$$u(r,0) = 0, v(r,0) = 0, r \in [0,1]\ ,$$
$$u(1,t) = 0, v(1,0) = 0, t > 0\ . \tag{10}$$

where $a_1 = \frac{1}{(1-\phi_n)-\phi_n\frac{\rho_s}{\rho_f}}$, $a_2 = \frac{a_1}{(1-\phi_n)^{2.5}}$, $a_3 = \sigma_f\left(1 + \frac{3(\sigma-1)\phi_n}{(\sigma+2)-(\sigma-1)\phi_n}\right), a_4 = a_1a_3$, $A_2 = a_1A_0$, $A_3 = a_1A_1$, $\beta_1 = a_2\left(1 + \frac{1}{\beta}\right)$ is the constant parameter, $R = a_1KN\left(\frac{{R_0}^2}{\mu_f}\right)$ is the particles concentration parameter, $Ha^2 = a_4\left(\frac{\sigma_f{R_0}^2B^2sin\theta}{\mu_f}\right)$ is the Hartman number, $F = \frac{\mu_f}{a_1gu_0R_0}$ is the inclination angle parameter and $G = \frac{mv}{K{R_0}^2}$ is the mass parameter of magnetic particles.

The Caputo-Fabrizio fractional derivative, NFD_t is defined as follows:

$$D_t^{\alpha}f(t) = \frac{M(\alpha)}{1-\alpha}\int_{\alpha}^{t}\exp\left(-\frac{\alpha(t-\tau)}{1-\alpha}\right)f'(\tau)\,d\tau \tag{11}$$

where, $0 < \alpha < 1$ and $M(\alpha)$ is a normalization function such as $M(0) = M(1) = 1$. From definition (11),

the Caputo-Fabrizio fractional derivative of a function equals to zero when $f(t)$ is a constant. The properties of non-singularities kernel provide a more flexible computation of a system, and its initial conditions can be interpreted in the classical sense, simplifying their incorporation in physical models. Besides, it helps to optimize the notion of differentiation to non-integer orders and available for intermediate derivatives that mode of phenomena with memory.

Solution Procedure

After implementing Laplace transform to the equations (8) and (9) along with the boundary conditions (10), the nanofluid flow model expressed such as:

$$\frac{s\bar{u}(r,s)}{s+\alpha(1-s)} = \frac{A_2}{s} + \frac{A_3 s}{s^2+\omega^2} + \beta_1\left[\frac{\partial^2\bar{u}(r,s)}{\partial r^2} + \frac{1}{r}\frac{\partial\bar{u}(r,s)}{\partial r}\right] + R[\bar{v}(r,s) - \bar{u}(r,s)] - Ha^2\bar{u}(r,s) + \frac{sin\phi}{sF}, \tag{12}$$

$$G \cdot \frac{s\bar{v}(r,s)}{s+\alpha(1-s)} = \bar{u}(r,s) - \bar{v}(r,s), \tag{13}$$

$$\bar{u}(1,s) = 0, \bar{v}(1,s) = 0. \tag{14}$$

From equation (13), we could derive the following equation:

$$\bar{v}(r,s) = \frac{s+\alpha(1-s)}{s+sG+\alpha(1-s)}\bar{u}(r,s)\,. \tag{15}$$

Substituting $\bar{v}(r,s)$ in equation (15) into equation (12) and rearrange them as following equation:

$$\bar{u}(r,s)\left[\frac{s}{s+\alpha(1-s)} - R\left(\frac{s+\alpha(1-s)}{s+sG+\alpha(1-s)}\right) + Ha^2 + R\right] = \frac{A_2}{s} + \frac{A_3 s}{s^2+\omega^2} + \frac{sin\phi}{sF} + \beta_1\left[\frac{\partial^2\bar{u}(r,s)}{\partial r^2} + \frac{1}{r}\frac{\partial\bar{u}(r,s)}{\partial r}\right]. \tag{16}$$

Applying finite Hankel transform with respect to the radial coordinate, r and considering the boundary conditions in (14), obtain:

$$\bar{u}_H(r_n,s)\left[\frac{s}{s+\alpha(1-s)} - R\left(\frac{s+\alpha(1-s)}{s+sG+\alpha(1-s)}\right) + Ha^2 + R\right] = \left[\frac{A_2}{s} + \frac{A_3 s}{s^2+\omega^2} + \frac{sin\phi}{sF}_1\right]\frac{J_1(r_n)}{r_n} - \beta {r_n}^2\bar{u}_H(r_n,s). \tag{17}$$

The expression $\bar{u}_H(r_n,s) = \int_0^1 r\bar{u}(r,s)J_0(r_n,s)dr$ represents the finite Hankel transform of the velocity function $\bar{u}(r,s) = \mathcal{L}[u(r,t)]$ and r_n,n=1,2,3,… are the positive roots of the equation $J_0(x) = 0$. In addition, J_0 represents the Bessel function of order zero and first kind. After derivation of the coefficient of $\bar{u}(r,s)$ in equation (17), the equation is:

$$\bar{u}_H(\varsigma_n,s) = \left[\frac{s^2y_{5n} + sy_{6n} + \alpha^2}{s^2y_{2n} + sy_{3n} + y_{4n}}\right]\left[\frac{1}{s}\left(A_2 + \frac{sin\phi}{F}\right) + \frac{A_3 s}{s^2+\omega^2}\right]\frac{J_1(r_n)}{r_n}. \tag{18}$$

By partial fractional to simply the coefficient in the righthand side of equation (18) and the simplified form is:

$$\bar{u}_H(r_n,s)=\left[\frac{y_{9n}}{s-y_{7n}}+\frac{y_{10n}}{s-y_{8n}}\right]\left[\frac{1}{s}\left(A_2+\frac{sin\phi}{F}\right)+\frac{A_3 s}{s^2+\omega^2}\right]\frac{J_1(r_n)}{r_n}. \tag{19}$$

The parameter in equation (18) and (19) introduced for simplifying the coefficient of $\bar{u}_H(r_n,s)$ are listed by:

$$y_{1n}=Ha^2+R+\beta_1 {r_n}^2,$$

$$y_{2n}=1+G-\alpha-R-R\alpha^2+2R\alpha+y_{1n}+\alpha^2 y_{1n}-2\alpha y_{1n}+Gy_{1n}-G\alpha y_{1n},$$

$$y_{3n}=\alpha+2R\alpha^2-2R\alpha-2\alpha^2 y_{1n}+2\alpha y_{1n}+G\alpha y_{1n},$$

$$y_{4n}=\alpha^2 y_{1n}-R\alpha^2,$$

$$y_{5n}=1+\alpha^2-2\alpha+G-G\alpha,$$

$$y_{6n}=-2\alpha^2+2\alpha+G\alpha,$$

$$y_{7n}=\frac{-y_{3n}+\sqrt{{y_{3n}}^2-4y_{2n}y_{4n}}}{2y_{2n}},$$

$$y_{8n}=\frac{-y_{3n}-\sqrt{{y_{3n}}^2-4y_{2n}y_{4n}}}{2y_{2n}},$$

$$y_{9n}=\frac{{y_{7n}}^2 y_{5n}+y_{7n}y_{6n}+\alpha^2}{y_{7n}-y_{8n}},$$

$$y_{10n}=\frac{{y_{8n}}^2 y_{5n}+y_{8n}y_{6n}+\alpha^2}{y_{8n}-y_{7n}}, \tag{20}$$

Expanding the coefficient of $\bar{u}_H(r_n,s)$ in equation (20) generates:

$$\bar{u}_H(r_n,s)=\left(A_2+\frac{sin\phi}{F}\right)\left[y_{9n}\frac{1}{s(s-y_{7n})}+y_{10n}\frac{1}{s(s-y_{8n})}\right]\frac{J_1(r_n)}{r_n}$$
$$+A_3\frac{s}{s^2+\omega^2}\left[y_{9n}\frac{1}{s-y_{7n}}+y_{10n}\frac{1}{s-y_{8n}}\right]\frac{J_1(r_n)}{\varsigma_n}. \tag{21}$$

The inverse Laplace transform of the image function $\bar{u}_H(r_n,s)$ in (21) is derived using the Robotnov and Hartley's functions:

$$u_H(r_n,t)=\frac{J_1(r_n)}{r_n}\left[(e^{y_{7n}t}-1)\left(\frac{A_2 y_{9n}}{y_{7n}}+\frac{y_{9n}sin\phi}{y_{7n}F}\right)+(e^{y_{8n}t}-1)\left(\frac{A_2 y_{10n}}{y_{8n}}+\frac{y_{10n}sin\phi}{y_{8n}F}\right)\right.$$
$$+\frac{y_{7n}}{{y_{7n}}^2+\omega^2}A_3 y_{9n}\left(e^{y_{7n}t}-\cos(\omega t)+\frac{w}{y_{7n}}\sin(\omega t)\right)$$
$$\left.+\frac{y_{8n}}{{y_{8n}}^2+\omega^2}A_3 y_{10n}\left(e^{y_{8n}t}-\cos(\omega t)+\frac{w}{y_{8n}}\sin(\omega t)\right)\right]. \tag{22}$$

The equation of the fluid flow velocity is formed by taking inverse Hankel transform of equation (22):

$$u(r,t) = 2\sum_{n=1}^{\infty} \frac{J_0\left(\frac{r}{R_z} r_n\right)}{J_1^2(r_n)} \times u_H(r_n, t), \tag{23}$$

$$\begin{aligned} u(r,t) = 2\sum_{n=1}^{\infty} \frac{J_0\left(\frac{r}{R_z} r_n\right)}{r_n J_1(r_n)} \Bigg[& (e^{y_{7n}t} - 1)\left(\frac{A_2 y_{9n}}{y_{7n}} + \frac{y_{9n} sin\phi}{y_{7n} F}\right) + (e^{y_{8n}t} - 1)\left(\frac{A_2 y_{10n}}{y_{8n}} + \frac{y_{10n} sin\phi}{y_{8n} F}\right) \\ & + \frac{y_{7n}}{{y_{7n}}^2 + \omega^2} A_3 y_{9n}\left(e^{y_{7n}t} - \cos(\omega t) + \frac{w}{y_{7n}} \sin(\omega t)\right) \\ & + \frac{y_{8n}}{{y_{8n}}^2 + \omega^2} A_3 y_{10n}\left(e^{y_{8n}t} - \cos(\omega t) + \frac{w}{y_{8n}} \sin(\omega t)\right)\Bigg]. \end{aligned}$$

(24)

Equation (24) represents the convolution product of *f* and *g*, denoted as $f * g$, which the product can computed as:

$$f * g(t) = \int_0^t f(\tau) g(t - \tau) d\tau. \tag{25}$$

The magnetic particle velocity is obtained from the equation (15):

$$v(r,t) = y_{12n}(1 - y_{11n})[u(r,t) * e^{y_{12n}t}], for\ 0 < \alpha < 1. \tag{26}$$

The new parameters involved in equation (26) are:

$$y_{11n} = \frac{1 - \alpha}{G - \alpha + 1}, \tag{27}$$

$$y_{12n} = \frac{\alpha}{G - \alpha + 1}. \tag{28}$$

Results and Discussion

To determine how various flow parameters affect blood flow velocity, u(r, t) and magnetic velocity, v(r, t), a proposed Mathcad solution is used to subsequent processing the analytical solutions in equations (24) and (26). The following parameters are fixed for the numerical simulation: $\phi_n = 0.025, A_0 = 0.1,\ A_1 = 0.1, G = 0.7, R = 0.5, \omega = \frac{\pi}{4}, t = 0.25,\ Ha = 1, and\ \beta = 0.4.$ After fixed these factors, the analytical solution of velocities were demonstrated graphically based on varying the Caputo-Fabrizio fractional flow parameters. Figure 2 - 5 display the impacts of 2 non-dimensional parameters such as Hartmann number, Ha and Casson fluid parameter, β, and order of fractional parameters and the time level, t. Also, Figure 1 presents the validation of the current model, where the case corresponding to $\alpha = 1$ is consistent with the findings reported in [33]. Furthermore, Table 1 shows the constant values of thermophysical properties of nanofluid [36, 37].

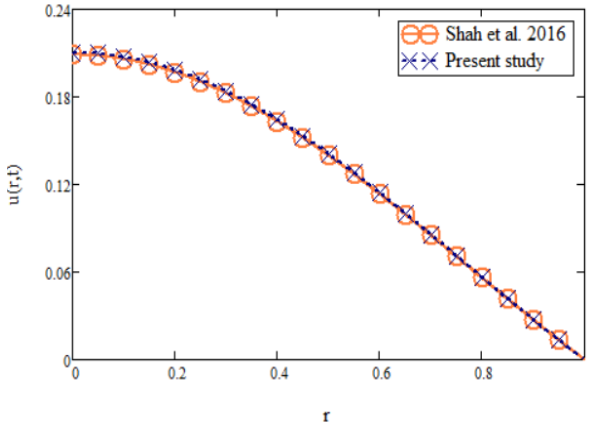

Figure 1. Comparison between [35] and present study for for $A_0 = 0.1$, $A_1 = 0.1$, $G = 0.7$, $R = 0.5$, $\omega = \frac{\pi}{4}$, $Ha = 1$, $t = 0.25$, $\beta = 0.4$, and $\alpha = 1.0$ against r.

Table 1 Thermophysical parameters of blood and Copper nanoparticles

Thermophysical properties	Blood	Copper
$\rho(kg/m^3)$	1063	8933
$c_p(J/kg\ K)$	3594	385
$K(W/mk)$	0.492	400
$\alpha(S/m)$	0.8	59.6 x10^6

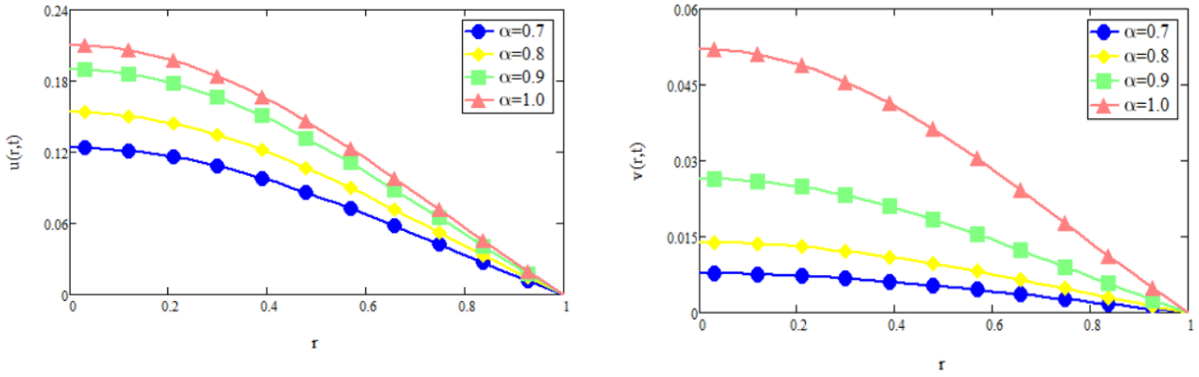

a) Blood flow velocity b) Magnetic particle velocity

Figure 2. Profile of axial velocities of $u(r,t)$ and $v(r,t)$ for $A_0 = 0.1$, $A_1 = 0.1$, $G = 0.7$, $R = 0.5$, $\omega = \frac{\pi}{4}$, $Ha = 1$, $t = 0.25$, $\beta = 0.4$, and $\alpha = 0.7$,0.8,0.9,1.0 against r.

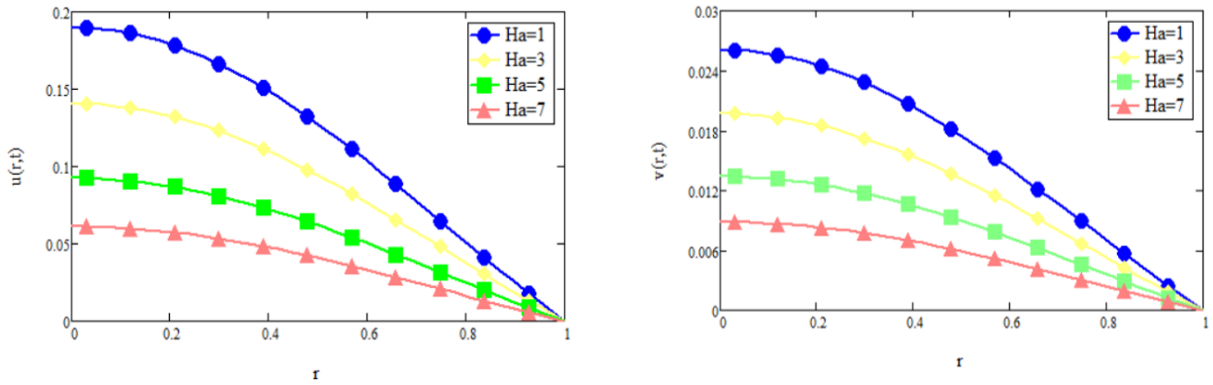

a) Blood flow velocity b) Magnetic particle velocity

Figure 3. Profile of axial velocities of $\mathrm{u}(\mathrm{r},\mathrm{t})$ and $\mathrm{v}(\mathrm{r},\mathrm{t})$ for $\mathrm{A}_0 = 0.1$, $\mathrm{A}_1 = 0.1$, $\mathrm{G} = 0.7$, $\mathrm{R} = 0.5$, $\omega = \frac{\pi}{4}$, $\alpha = 0.9$, $\mathrm{t} = 0.25$,$\beta = 0.4$, and $\mathrm{Ha} = 1,3,5,7$ against r.

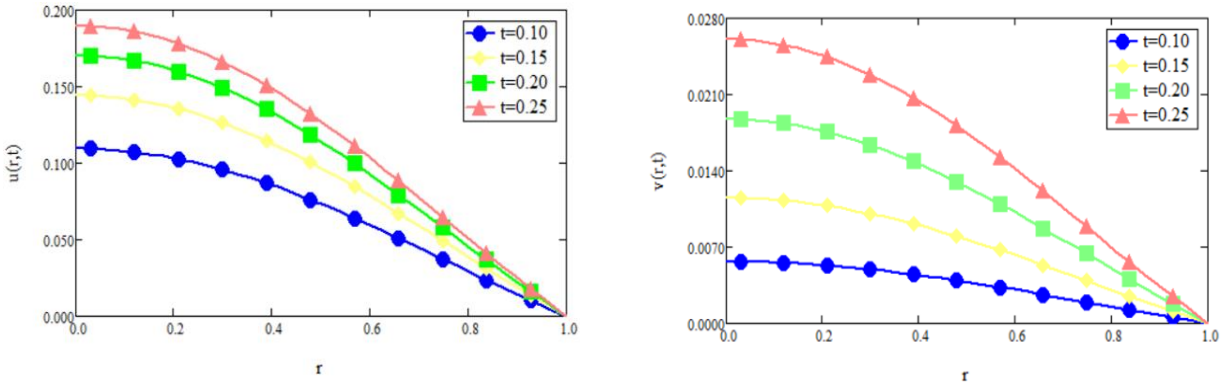

a) Blood flow velocity b) Magnetic particle velocity

Figure 4. Profile of axial velocities of $u(r,t)$ and $v(r,t)$ for $A_0 = 0.1$, $A_1 = 0.1$, $G = 0.7$, $R = 0.5$, $\omega = \frac{\pi}{4}$, $\alpha = 0.9$, $Ha = 1$, $\beta = 0.4$, and $t = 0.10,0.15,0.20,0.25$ against r.

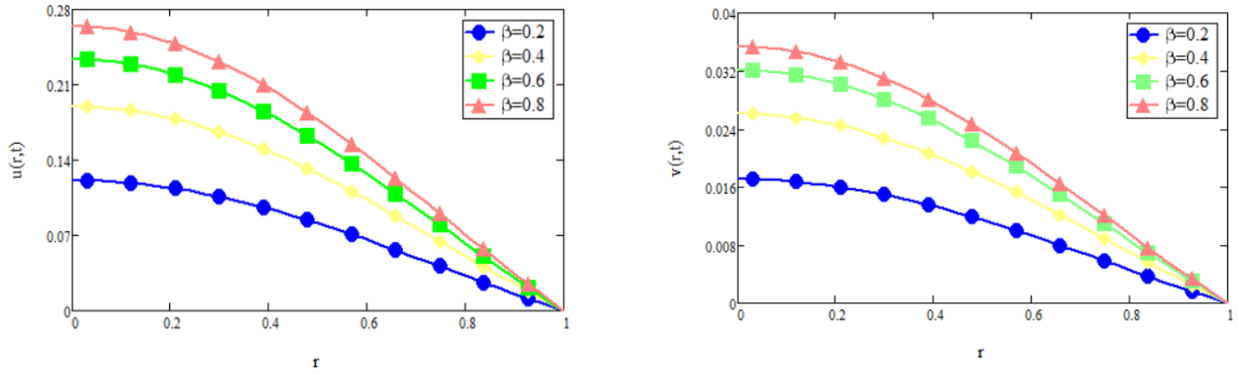

a) Blood flow velocity b) Magnetic particle velocity

Figure 5. *Profile of axial velocities of* $u(r,t)$ *and* $v(r,t)$ *for* $A_0 = 0.1$, $A_1 = 0.1$, $G = 0.7$, $R = 0.5$, $\omega = \frac{\pi}{4}$, $\alpha = 0.9$, $Ha = 1$, $t = 0.25$, *and* $\beta = 0.2,0.4,0.6,0.8$ *against r.*

The impact of fractional parameters ($\alpha = 0.7,0.8,0.9,1.0$) on the targeted velocities is depicted in Figure 2. An increase in the fractional parameter, α results in higher velocities for both blood flow and magnetic particles, with the blood flow velocity exhibiting a greater magnitude. A lower fractional order indicates a stronger memory effect in the fluid and cause a damping force. Consequently, the result suggests that the classical blood flow model predicts higher velocities compared to the Casson fluid model incorporating fractional derivatives.

Figure 3 shows the inverse relationship between the Hartmann number and both velocities. Consequently, the magnetic field is observed to significantly reduce the axial velocities of blood and magnetic particles. This is because a higher Hartmann number implies a stronger magnetic field effect that will produce a stronger Lorentz force, which acts as resistive force that opposes the fluid motion.

A positive correlation is observed between the time level and velocity profile, as illustrated in Figure 4. The system gains momentum under driving pressure gradient and cause fluid accelerates from initial condition to higher time level. Thus, the study reveal that the time level has significant impact on controlling the distribution of blood flow.

Changes in the Casson parameter (β) which denotes the yield stress of the Casson fluid are illustrated in Figure 5. Here, high β values of the Casson parameter result in increased velocities for both components. Since the Casson parameter is inversely proportional to the fluid's viscosity, an increment of the Casson parameter leads to lowering the effective viscosity and internal resistance. Consequently, fluid can flow faster as the Casson parameter increases. The result is aligned with previous findings of Azmi, *et al*. [20] and Ali, *et al*. [30].

Conclusions

Considering all the variables, a mathematical model has been developed to analyze the magnetic Casson blood flow with copper nanoparticles through an inclined stenosed artery in order of fractional time derivatives. The final governing equation is symbolized as Caputo-Fabrizio time fractional derivatives with the order range for (0,1]. Both analytical methods, Laplace and finite Hankel transforms were implied to obtain the analytical solutions for velocities between blood flow and magnetic particles. Application of software, Mathcad generated the graph based on varying of parameters. From the graphical results,

1. The application of magnetic field markedly suppresses the axial motion of blood and magnetic particles.
2. The velocity of blood flow and magnetic particle is positively correlated with an increase in fractional order, time and Casson fluid parameters.
3. Generally, the velocity of blood flow is higher than the magnetic particle velocity.

These results could help medical professionals predict patient outcomes in cases of arterial stenosis based on activity levels and the location of the narrowing. Future studies should consider employing different fluid models and diverse arterial conditions.

Conflicts of Interest

The authors declare that there is no conflict of interest regarding the publication of this paper.

Acknowledgement

This research was funded by the Universiti Teknologi Malaysia (UTM) under UTM Potential Academic Staff grant Vote No.: Q.J130000.2754.04K09.

References

[1] Akbar, N. S. (2014). Blood flow analysis of Prandtl fluid model in tapered stenosed arteries. *Ain Shams Engineering Journal, 5*(4), 1267–1275.
[2] Kallekar, L. C., Viswanath, M., & Anand, M. (2017). Effect of wall flexibility on the deformation during flow in a stenosed coronary artery. *Fluids, 2*(2), 16. https://doi.org/10.3390/fluids2020016.
[3] Beckman, J. A., Ansel, G. M., Lyden, S. P., & Das, T. S. (2020). Carotid artery stenting in asymptomatic carotid artery stenosis: JACC review topic of the week. *Journal of the American College of Cardiology, 75*(6), 648–656. https://doi.org/10.1016/j.jacc.2019.12.040.
[4] Dhange, M. G., Sankad, U., Bhujakkanavar, K. K., & Misra, J. C. (2024). Hemodynamic characteristics of blood flow in an inclined overlapped stenosed arterial section. *Partial Differential Equations in Applied Mathematics, 11*, 100829. https://doi.org/10.1016/j.padiff.2024.100829.
[5] Udupa, M. C., Saha, S., & Natarajan, S. (2025). Study of blood flow patterns in a stenosed artery through the combined effect of body acceleration and generalized Womersley solution. *Scientific Reports, 15*(1), 1845. https://doi.org/10.1038/s41598-025-01845-x.
[6] Sharma, B., Gandhi, R., Abbas, T., & Bhatti, M. M. (2023). Magnetohydrodynamics hemodynamics hybrid

nanofluid flow through inclined stenotic artery. *Applied Mathematics and Mechanics, 44*, 459–476. https://doi.org/10.1007/s10483-023-2923-0.
[7] Intan Diyana, M., Nurul Aini, J., & Sharidan, S. (2023). Solute dispersion in an unsteady Herschel–Bulkley flow through an inclined stenosed artery. *Journal of Advanced Research in Numerical Heat Transfer, 14*(1), 29–38.
[8] Bali, R., & Awasthi, U. (2007). Effect of a magnetic field on the resistance to blood flow through stenotic artery. *Applied Mathematics and Computation, 188*, 1635–1641. https://doi.org/10.1016/j.amc.2006.11.012
[9] Ikbal, M. A., Chakravarty, S., Wong, K. L., Mazumdar, J., & Mandal, P. K. (2009). Unsteady response of non-Newtonian blood flow through a stenosed artery in magnetic field. *Journal of Computational and Applied Mathematics, 230*(1), 243–259. https://doi.org/10.1016/j.cam.2009.01.031.
[10] Zainal, N. A., Nazar, R., Naganthran, K., & Pop, I. (2021). Stability analysis of unsteady MHD rear stagnation point flow of hybrid nanofluid. *Mathematics, 9*(19), 2428. https://doi.org/10.3390/math9192428.
[11] Zainal, N. A., Nazar, R., Naganthran, K., & Pop, I. (2021). Unsteady MHD mixed convection flow in hybrid nanofluid at three-dimensional stagnation point. *Mathematics, 9*(5), 549. https://doi.org/10.3390/math9050549.
[12] Varshney, G., Katiyar, V., & Kumar, S. (2010). Effect of magnetic field on the blood flow in artery having multiple stenosis: A numerical study. *International Journal of Engineering, Science and Technology, 2*(2), 967–982.
[13] Mamun, K., Funazaki, K., Akter, S., & Akhter, M. (2020). The effect of magnetic field on blood flow through stenotic artery: A review on biomagnetic fluid dynamics.
[14] Liaqat, H., Salah, U., & Asif, S. (2023). Unsteady and incompressible magnetohydrodynamics blood flow in an inclined cylindrical channel. *International Journal of Physics Research and Applications*.
[15] Wajihah, S. A., & Sankar, D. S. (2023). A review on non-Newtonian fluid models for multi-layered blood rheology in constricted arteries. *Archive of Applied Mechanics, 93*(5), 1771–1796. https://doi.org/10.1007/s00419-023-02368-6.
[16] Akhtar, S., Hussain, Z., Nadeem, S., Najjar, I. M. R., & Sadoun, A. M. (2023). CFD analysis on blood flow inside a symmetric stenosed artery: Physiology of coronary artery disease. *Science Progress, 106*(2), 368504231180092. https://doi.org/10.1177/00368504231180092.
[17] Buchanan, J. R., Kleinstreuer, C., & Comer, J. K. (2000). Rheological effects on pulsatile hemodynamics in a stenosed tube. *Computers & Fluids, 29*(6), 695–724. https://doi.org/10.1016/S0045-7930(99)00033-4.
[18] Siddiqui, S. U., Verma, N. K., Mishra, S., & Gupta, R. S. (2009). Mathematical modelling of pulsatile flow of Casson's fluid in arterial stenosis. *Applied Mathematics and Computation, 210*(1), 1–10. https://doi.org/10.1016/j.amc.2008.12.059.
[19] Azmi, W. F. W., Mohamad, A. Q., Jiann, L. Y., & Shafie, S. (2021). Analytical solution of unsteady Casson fluid flow through a vertical cylinder with slip velocity effect. *Journal of Advanced Research in Fluid Mechanics and Thermal Sciences, 87*(1), 68–75.
[20] Bhatti, M. M., Sait, S. M., & Ellahi, R. (2022). Magnetic nanoparticles for drug delivery through tapered stenosed artery with blood-based non-Newtonian fluid. *Pharmaceuticals, 15*(11), 1352. https://doi.org/10.3390/ph15111352.
[21] Majeed, S., Ali, F., Imtiaz, A., Khan, I., & Andualem, M. (2022). Fractional model of MHD blood flow in a cylindrical tube containing magnetic particles. *Scientific Reports, 12*(1), 418. https://doi.org/10.1038/s41598-021-04088-9
[22] Choi, S. U. S., & Eastman, J. A. (1995). Enhancing thermal conductivity of fluids with nanoparticles.
[23] Elnaqeeb, T., Mekheimer, K. S., & Alghamdi, F. (2016). Cu-blood flow model through a catheterized mild stenotic artery with a thrombosis. *Mathematical Biosciences, 282*, 135–146. https://doi.org/10.1016/j.mbs.2016.10.005.
[24] Maqbool, K., Shaheen, S., & Siddiqui, A. M. (2019). Effect of nanoparticles on MHD flow of tangent hyperbolic fluid in a ciliated tube: An application to fallopian tube. *Mathematical Biosciences and Engineering, 16*(4), 2927–2941. https://doi.org/10.3934/mbe.2019147.
[25] Awadalla, M., Abuasbeh, K., Noupoue, Y.-Y.-Y., & Abdo, M.-S. (2023). Modeling drug concentration in blood through Caputo–Fabrizio and Caputo fractional derivatives. *Computer Modeling in Engineering & Sciences, 135*(3), 2767–2785. https://doi.org/10.32604/cmes.2023.026148.
[26] Abbas, S., Nisa, Z. U., Nazar, M., Amjad, M., Ali, H., & Jan, A. Z. (2024). Application of heat and mass transfer to convective flow of Casson fluids in a microchannel with Caputo–Fabrizio derivative approach. *Arabian Journal for Science and Engineering, 49*(1), 1275–1286. https://doi.org/10.1007/s13369-023-08351-1.
[27] Caputo, M., & Fabrizio, M. (2015). A new definition of fractional derivative without singular kernel. *Progress in Fractional Differentiation and Applications, 1*, 73–85.
[28] Ali, F., Imtiaz, A., Khan, I., & Sheikh, N. A. (2018). Flow of magnetic particles in blood with isothermal heating: A fractional model for two-phase flow. *Journal of Magnetism and Magnetic Materials, 456*, 413–422. https://doi.org/10.1016/j.jmmm.2018.02.038.
[29] Moitoi, A. J., & Shaw, S. (2022). Magnetic drug targeting during Caputo–Fabrizio fractionalized blood flow through a permeable vessel. *Microvascular Research, 139*, 104262. https://doi.org/10.1016/j.mvr.2021.104262.
[30] Yadeta, H. B., & Shaw, S. (2023). Analysis of unsteady non-Newtonian Jeffrey blood flow and transport of magnetic nanoparticles through an inclined porous artery with stenosis using the time fractional derivative. *Journal of Applied Physics, 134*(10), 104701. https://doi.org/10.1063/5.0161926.
[31] Mackolil, J., & Mahanthesh, B. (2019). Exact and statistical computations of radiated flow of nano and Casson fluids under heat and mass flux conditions. *Journal of Computational Design and Engineering, 6*(4), 593–605. https://doi.org/10.1016/j.jcde.2019.04.005.
[32] Jamil, D. F., Uddin, S., Kamardan, M. G., & Roslan, R. (2020). The effects of magnetic blood flow in an inclined cylindrical tube using Caputo–Fabrizio fractional derivatives. *CFD Letters, 12*, 111–122.
[33] Shah, N. A., Vieru, D., & Fetecau, C. (2016). Effects of the fractional order and magnetic field on the blood flow in cylindrical domains. *Journal of Magnetism and Magnetic Materials, 409*, 10–19. https://doi.org/10.1016/j.jmmm.2016.02.049.
[34] Khashi'ie, N. S., Arifin, N. M., Pop, I., & Wahid, N. S. (2020). Flow and heat transfer of hybrid nanofluid over a permeable shrinking cylinder with Joule heating: A comparative analysis. *Alexandria Engineering Journal, 59*(3), 1787–1798. https://doi.org/10.1016/j.aej.2020.04.021.

[35] Noranuar, W. N. I. N., Mohamad, A. Q., Shafie, S., Khan, I., Jiann, L. Y., & Ilias, M. R. (2021). Non-coaxial rotation flow of MHD Casson nanofluid carbon nanotubes past a moving disk with porosity effect. *Ain Shams Engineering Journal, 12*(4), 4099–4110. https://doi.org/10.1016/j.asej.2021.03.009.
[36] Khashi'ie, N. S., Arifin, N. M., Pop, I., & Wahid, N. S. (2020). Flow and heat transfer of hybrid nanofluid over a permeable shrinking cylinder with Joule heating: A comparative analysis. *Alexandria Engineering Journal, 59*(3), 1787–1798. https://doi.org/10.1016/j.aej.2020.04.021.
[37] Noranuar, W. N. I. N., Mohamad, A. Q., Shafie, S., Khan, I., Jiann, L. Y., & Ilias, M. R. (2021). Non-coaxial rotation flow of MHD Casson nanofluid carbon nanotubes past a moving disk with porosity effect. *Ain Shams Engineering Journal, 12*(4), 4099–4110. https://doi.org/10.1016/j.asej.2021.03.009.